Biogeosciences Discuss., 11, 14667–14698, 2014
www.biogeosciences-discuss.net/11/14667/2014/
doi:10.5194/bgd-11-14667-2014

Biogeosciences
Discussions
Open Access

Modelling forest lines and forest distribution patterns with remote sensing data in a mountainous region of semi-arid Central Asia

M. Klinge[1], J. Böhner[2], and S. Erasmi[1]

[1]Institute of Geography, University of Göttingen, Goldschmidtstr. 5, 37077 Göttingen, Germany
[2]Institute of Geography, University of Hamburg, Bundesstraße 55, 20146 Hamburg, Germany

Received: 17 July 2014 – Accepted: 25 September 2014 – Published: 13 October 2014

Correspondence to: M. Klinge (mklinge1@gwdg.de)

Published by Copernicus Publications on behalf of the European Geosciences Union.

Abstract

Satellite images and digital elevation models provide an excellent database to analyse forest distribution patterns and forest limits in the mountain regions of semi-arid Central Asia at the regional scale. For the investigation area in the northern Tien Shan a strong relation between forest distribution and climate conditions could be found. Additionally areas of potential human impact on forested areas are identified at lower elevations near the mountain border based on an analysis of the differences of climatic preconditions and present occurrence of forest stands.

The distribution of spruce (*Picea schrenkiana*) forests is hydrologically limited by a minimum annual precipitation of 250 mm and thermally by a minimum monthly mean temperature of 5 °C during the growing season. While the actual lower forest limit increases from 1600 m a.s.l. in the northwest to 2600 m a.s.l. in the southeast, the upper forest limit takes the same course from 1800 to 2900 m a.s.l. In accordance with the main wind directions, the steepest gradient of both forest lines and the greatest local vertical extent of the forest belt of 500 to 600 m and maximum 900 m occur at the northern and western mountain fronts.

The forests in the investigation area are strongly restricted to north facing-slopes, which is a common feature in semi-arid Central Asia. Based on the presumption that variations in local climate conditions are a function of topography, the potential forest extent was analysed with regard to the parameters slope, aspect, solar radiation input and elevation. All four parameters showed a strong relationship to forest distribution, yielding a total potential forest area that is 3.5 times larger than the present forest remains of 502 km^2.

1 Introduction

The latitudinal and elevational variation of distinct plant associations and geomorphologic landscape units has been used for a long-time to deduce regional environmental and climatically conditions in geosciences (e.g. Humboldt, 1845–1862; Troll, 1973a, b; Hövermann, 1985). Image classification and GIS-modelling of remote sensing data are standard methods to map landscape elements and their distribution in remote areas, which are poorly accessible due to logistic or political difficulties. Satellite analysis based on automated image processing offers a quick and beneficial alternative to field mapping or manual digitalisation from aerial image (Mayer and Bussemer, 2001). While satellite images like Landsat-data provide excellent information to delineate the spatial forest distribution (Hansen et al., 2013), SRTM-data can be used to examine relief dependent distribution patterns with a digital terrain model (DTM). The combination of these two data sets enables high resolution mapping at regional to local scale.

The geoecologic and climatic environmental settings control the natural distribution of forest stands (Holtmeier, 2000; Körner, 2012; Miehe et al., 2003). In addition, the actual situation can strongly be influenced by human activities like logging, fire clearing and animal grazing, which decreases the potential natural forest area (PFA). This often makes it difficult to differentiate between natural factors and human impact on the distribution of timbered areas. In general, human activity has reduced the forest area since prehistorically times so that the actual forest area (AFA) pattern represents the minimum of the potential environmental distribution range. Due to the highly continental, cold and dry climate in semi-arid Central Asia, tree growth is mostly restricted to topography parameters. Forest stands beyond groundwater favoured sites are predominantly limited to north-facing slopes in the mountains with an upper and lower forest limit (Dulamsuren et al., 2014; Hilbig, 1995; Klinge et al., 2003; Treter, 1996, 2000).

Different definitions have been used for tree- and forest lines (Körner, 2012; Körner and Paulsen, 2004). The treeline ecotone covers three main boundary lines at the upper forest distribution limit. The highest is the tree species line, where tree seedlings

BGD
11, 14667–14698, 2014

occur but no adult trees. The treeline is the maximum elevation where patches of forest can exist at topographic favoured places. In our investigation we refer to the forest line, which is defined as the limit of closed forest at the upper (timberline) and lower boundary of forest distribution.

For the region of northern Tien Shan in China, Dai et al. (2013) state an upper forest line beginning with 2900 m a.s.l. in the west, which decreases eastward down to 2500 m a.s.l. and then rises again to 2900 m a.s.l. in the east. In the north-western Tien Shan Fickert (1998) reports an upper forest line of 2900 and 2850 m a.s.l. and a lower forest line of 2400 and 2500 m a.s.l., respectively for the Sailijski-Alatau and Kungeij-Alatau. In the Altay Mountains Klinge et al. (2003) found upper forest lines increasing eastward from 1800 to 2600 m a.s.l. and lower forest lines concurrently increasing from 1000 to 2200 m a.s.l. while the vertical extension of the forest belt varies between 400 and 1200 m.

Tree growth in high mountains is generally restricted by temperature conditions (Haase et al., 1964; Holtmeier, 2000; Jobbagy and Jackson, 2000; Körner, 2012). The upper forest line is a thermal determined distribution boundary that is generally defined by the mean July temperature (Walter and Breckle, 1994) or the warmest month isotherm of 10 °C. According to Körner (2012) and Körner and Paulsen (2004) this parameter is not suitable in all parts of the world. This can be seen in Fickert (1998), who shows that the upper forest line in the northern Tien Shan coincides well with the 10 °C July-isotherm, while further south in NW-Himalaya and NW-Karakorum it is connected to the July-isotherms of 16 and 12 °C, respectively. For the eastern side of the northern Tien Shan Dai et al. (2013) report a mean temperature of the warmest month of 10.5 °C at the mean position of the alpine forest line. Also the mean annual air temperature (MAAT) is weakly correlated to the forest line because it includes temperatures from the non-growing season which play a minor role for tree growth (Jobbagy and Jackson, 2000; Körner, 2012).

A suitable way to describe the temperature environment at the upper forest line is a minimum threshold value for the mean air temperature during the growing season

BGD
11, 14667–14698, 2014

which is defined as the period of monthly mean temperatures above 5 °C (Dai et al., 2013; Körner, 2012; Körner and Paulsen, 2004). Based on the strong correlation between soil and air temperatures, Körner and Paulsen (2004) state a global range of 5.5 to 7.5 °C for minimum mean air temperature during the growing season. Paulsen and Körner (2014) developed a climate-based model for treeline prediction by defining the growing season as days with mean temperature above 0.9 °C and a mean temperature of more than 6.4 °C during that time. For the upper forest line between 2750 and 2920 m a.s.l. in the Tien Shan Mountains in Kyrgyzstan Körner (2012) found a mean temperature of 6.5 °C during the 155 days of the growing season (late April until late September).

The forest expansion into dry regions is controlled by precipitation and soil water supply (Dulamsuren et al., 2010, 2014; Kastner, 2000; Klinge et al., 2003). Between the more humid mountain regions and the arid basins of Central Asia a lower limit of forest distribution occurs which is termed the lower forest line. According to Walter and Breckle (1994) this forest distribution boundary coincides with an annual precipitation of at least 300 mm, while Holdridge (1947) proposes 250 mm and Miehe et al. (2003) found *Juniperus* trees in southern Tibet growing in regions with annual precipitation between 200 and 250 mm. Dulamsuren et al. (2010) state an annual precipitation between 230 and 400 mm at lower elevations for larch forests in northern and central Mongolia. In western Mongolia Dulamsuren et al. (2014) found coniferous forests existing at annual precipitation near 120 mm, which are explained by soil water benefits due to the occurrence of permafrost ice in the soil.

Everywhere in mountainous areas of the semi-arid Inner Asian forest-steppe coniferous forests are restricted to north facing slopes. While the north-facing slopes are dominated by larch trees *(Larix sibirica)* in Mongolia, spruce trees *(Picea schrenkiana)* occur in the Tien Shan Mountains (Dai et al., 2013; Fickert, 1998; Liu et al., 2013; Wang, 2005, 2006). Thus the restriction of conifers to north-facing slopes in the Inner Asian forest-steppe is not bound to certain tree species but rather to the environmental settings.

BGD
11, 14667–14698, 2014

The semi-arid climate conditions generate an overall deficiency of moisture which considerably influences the elevational forest distribution and may even control the upper forest limit (Liang et al., 2012; Liu et al., 2013; Miehe et al., 2008). A specific relief position is combined with particular climate conditions like temperature, precipitation, evaporation and insulation, which are similar at comparable sites in the surroundings. For this reason the relief parameters elevation, aspect, slope angle and solar radiation input can be used to define topoclimatic conditions in mountain regions (Miehe et al., 2003). However, a transfer of potential forest sites based on those definitions, the geologic and soil properties have to be comparable.

The impact of human activity on vegetation and especially on the forest since prehistorically times is a permanent question that needs to be proofed to clarify the environmental significance of any actual forest line (Miehe and Miehe, 2000). Dulamsuren et al. (2014) found a considerable anthropo-zoogenic influence on the actual lower forest line in the Mongolian Altai. For northern Mongolia Schlütz et al. (2008) showed that the present vegetation pattern in the mountain taiga where steppes occur on south-facing slopes is caused by climate conditions and relief, and is not originating from human activities.

Human impact on natural forests in Kazakhstan goes back to prehistoric times with nomadism and animal grazing as lifestyle adapted to the natural framework of the steppe (Karger, 1965; Giese, 1981, 1983). During summertime the alpine meadows and mountain steppes in the upper mountains were regularly used as pastures for the livestock. Even during Soviet times in Kazakhstan the nomadic movements were generally adopted by the Sowchos-System. Until today the alpine pastures are still in use. Extensive animal grazing prohibits the rejuvenation of trees and nomads may expand the grassland by fire setting.

Spatial models, which are able to predict the climatically induced forest distribution and especially the upper forest line on a global scale by exclusively using spatial climate data already exist (Paulsen and Körner, 2014). However, a clear method to empirically distinguish the actual forest distribution and its elevational limits for small areas covering a single mountain system and to simultaneously proof the potential human impact is lacking. In this investigation we introduce a procedure to solve this problem based on medium resolution remote sensing data. In addition, spatially explicit climate data and tree growth limiting climate parameters serve to differentiate potential human impact from natural conditions in the forest distribution.

2 Study area

The detailed investigation area Uzynkara ridge or Ketmen mountain range is located in the northernmost part of the Tien Shan Mountains in Central Asia at the border between Kazakhstan and China (79–81° E/42°45′–43°45′ N) (Fig. 1). Main cities are Shonzy and Kegen. The complete mountain range is part of the catchment area (CA) of the Ili river in the north. While the northern mountain side is directly drained to the Ili river, the Kegen river in the southern intermountain basin first flows westward and then turns as Sharyn river into a northern direction, and the Tekes river in the southernmost part runs eastward to Chinese territory. The mountain system is structured by two main ridges, a northern front range (NFR) and a southern mountain range (SMR), which converge in the east and enclose an intermountain basin in the west. A planation surface occurs in 3400 m a.s.l. and the highest peak is the Nebesnaja reaching 3652 m a.s.l. North facing Pleistocene cirques are cut into the high mountain plateau, where today no glaciation but permafrost occurs. The mountain border is tectonically clearly accentuated against the alluvial fans and fanglomerats in approximately 1500 m a.s.l. in the North and in 2000 m a.s.l. in the southern intermountain basin following west to east trending fault lines. The mountains mainly consist of metamorphic and volcanic Carboniferous and Devonian rocks including several Palaeozoic granite bodies. Locally also Permian, Silurian and Jurassic rocks are distributed.

The MAAT in Almaty (848 m a.s.l.) is 8.7 °C and in Karakol (1744 m a.s.l.) which is situated south of the investigation area 6.3 °C, respectively (Fickert, 1998). According to Medeu (2010) the mean air temperature is between −8 and −10 °C in January and

BGD
11, 14667–14698, 2014

between 20 and 24 °C in July. In wintertime the Siberian anticyclone produces weather conditions with cold air masses in the basins and warmer air temperatures above the inversion layer between 1000 and 1550 m a.s.l. (Giese, 1973).

The majority of precipitation in Kazakhstan comes along with air masses from western and south-western directions. In the mountains of northern Tien Shan mainly convective rainfall occurs in spring and autumn. Additionally cold air masses from northern directions bring precipitation to the northern Tien Shan in summertime (Böhner, 2006; Lydolph, 1977). According to Giese (1973) the annual precipitation in the basins of the foreland lies between 100 and 300 mm, in the lower mountains and in the intermountain basin it is between 300 and 400 mm. In the mountains it increases to more than 800 mm. The precipitation maxima occur in Mai, June, and subordinate in September.

The foreland, basins, and treeless mountain areas are covered by steppe vegetation with forb and bunch grass (Medeu, 2010). To the drier regions in the north it changes to grassland, sagebrush desert, saltwort, and sedge vegetation. The forest belt mainly consists of spruce trees (*Picea schrenkiana*). In the westernmost part aspen trees (*Populus tremula*) and in the northeastern part birch trees (*Betula pendula*) additionally occur. On the southern slopes shrub areas exist also.

The soils are distributed according to the climate conditions and the vegetation zones (Medeu, 2010). In the foreland desert soils occur. In the lower front ranges and in the intermountain basin mountain steppe soils of castanozem and chernozem type are distributed. In the forest belt dark chernozems which are locally bleached and podzolized occur under forest and pheaozem soils exist at meadow steppe sites. In the high elevations alpine and subalpine soils occur with mountain meadows and meadow steppes.

Arable land in eastern Kazakhstan is located in front of the mountain ranges on the alluvial fans in the basins and on the foothills in lower elevation. In this transition zone between the pediments and mountain ranges the soils are improved by a content of Pleistocene loess (Giese, 1983; Karger, 1965; Machalett et al., 2006). In front of the mountain border, the rivers spend the water for irrigation cultivation on the pediments.

BGD
11, 14667–14698, 2014

On the foothills agriculture is supported by sufficient rainfall as the so-called “Bogar”-Cultivation (Giese, 1983). According to these requirements the settlements are located along main valleys at the mountain boundary. Around the settlements wood-cutting is pronounced for construction and fuel.

3 Methods

A schematic workflow of the GIS-analysis procedure with input data, intermediate data, and output data is presented in Fig. 2. The analysis is divided into two main processes: the first is working on the relief parameters to estimate the PFA and the second conducts the delineation of the upper and lower forest lines. The forest lines are defined as the distribution boundaries of closed forest stands with areas larger than 0.5 ha, disregarding single trees which may represent special environmental places or remnants of former forests. Trees near the rivers of the valley bottoms were excluded from the examination because these are groundwater favoured sites which are mostly occupied by deciduous trees.

The determination of the AFA in the investigation area was performed by a supervised classification method based on a multispectral satellite image (visible light and infrared channels) from Landsat 7/ETM+ of the 13 September 2000 (Fig. 3). Aerial photos provided as imagery and bing basemaps by ESRI served for accuracy control. Depending on the ground resolution of 30 m × 30 m one pixel covers the occurrence of several individual trees so that small clearings and aisles could have been disregarded.

The relief parameters elevation, aspect, slope gradient, and total solar radiation input were derived from a DTM based on SRTM-data (Rabus et al., 2003), which was converted to an UTM-zone 44 north projection with a spatial resolution of 90 to 90 m. The polygons of the delineated forest stands were intersected with the relief parameters in order to investigate the relief dependent spatial distribution of forest sites in the study area. In addition, the statistics of all relief parameters were computed for the total study area (TSA) to indicate the potential impact of topography on the spa-

BGD
11, 14667–14698, 2014

tial distribution of forest stands (Fig. 4). Based on the assumption that at those places where all four relief parameters are within a distinct range, which was found responsible for forest distribution, the PFA was identified. This range was defined by the SD (standard deviation) (95 %) from single frequency distribution of the relief parameters aspect, slope gradient, and sum of solar radiation input during the mean growing season (March to November). While these parameters are not systematically influenced by human impact, the vertical distribution may have been changed by forest clearing at the lower and upper boundary. Therefore 99 % of the frequency distribution of the elevation parameter was chosen in this case.

Baseline climate data sets for Central Asia, comprising monthly radiation, temperature and precipitation data in a horizontal resolution of 0.5 arc seconds (approximately 1200 m in longitudinal and 850 m in latitudinal direction) are provided by Böhner (2006). The regular-grid climate layers were estimated using an empirical modelling approach, which basically integrates statistical downscaling of coarse resolution atmospheric fields (NCAR/NCEP-CDAS reanalyses series) and GIS based surface parameterization techniques, to sufficiently account for the topographic heterogeneity of the target area. A comprehensive description of data bases and modelling techniques is given in Böhner (2006) and Böhner and Antonic (2008). The suitability and precision of the modelling approach is discussed in Gerlitz et al. (2013) and Soria-Auza et al. (2010).

The frequency distribution of selected climate parameters related to the AFA and the TSA shown in Fig. 5 was calculated in the same way as described above. In contrast to the high resolution of the SRTM-data the climate data has a resolution about 10 times lower which leads to a generalisation and coarser scale of relief positions, where climatic differences between slope aspects inside the valleys are averaged. The climate data related to the forest stands is analysed by the climatic limitation values for forest development to detect potential human impact on the forest distribution patterns when obvious discrepancies occur.

To outline the actual forest lines it is initially necessary to segment the relief into small CAs, which represent small side-valleys or slope niches divided by convex ridges. This is done by computing the surficial hydrology regime from the DTM. The size of a CA is given by the threshold value for the stream definition function, which assigns the minimum number of cells to discharge into a specific cell to start a depth contour. In this study a value of 200 was found practical for the lower forest line and a value of 100 was suitable for the upper forest line. The single CAs generally consist of a part from the left and right side of a valley. Having different aspects in one segment is expedient to receive a general forest line value for one valley section.

After combining the catchment polygons with the forest polygons it is possible to determine the maximum and minimum elevation values for forests inside a single CA. The calculated values are spatially allocated as points to the position of those pixels which have the determined forest line value. To eliminate the preconditions on the lower forest line given by the elevation limits of the relief only those minimum values of forest stands were chosen, which are more than 50 m higher as the total minimum value of the CA. The distance between the highest forest stands and the crest line above has a special influence on the upper forest line which is called the "summit syndrome" by Körner (2012). Near the summits the local climate conditions strongly suppress tree growth by stronger wind, reduced temperature and snow drift. To receive a reasonable value for the climatic upper forest line and to eliminate preconditions by relief height, only those maximum forest values were chosen which lie more than 100 m below the total maximum elevation of the catchment. Finally, the forest lines were calculated from the remaining points by a natural neighbour interpolation method.

BGD
11, 14667–14698, 2014

4 Results

4.1 Relief parameterisation

The total AFA in the investigation area is 502 km^2 (Fig. 3). Frequency distributions of relief parameters for the AFA are shown in Fig. 4. The slope gradient and solar radiation of the forest stands show a normal distribution. The values with maximum distribution are 28° for slope gradient and 1075 $kWh\,m^{-2}$ for the sum of solar radiation input (Table 1). Less than 5 % of the forests exist on southern slopes (SE-S-SW). The curve of the parameter aspect has a steeper left slope and a maximum value in the north-western direction (315°), which is strongly related to the diurnal air temperature trend caused by insolation and heating processes on different slope directions. This underlines the fact that the strong relation of forest distribution to slope aspect is caused by natural environmental conditions. The curve of the parameter elevation has a shallow left slope, which may indicate human impact on forest distribution by wood cutting at the lower boundary. The lower forest lines start at 1575 m a.s.l. and the upper forest lines exceed 2900 m a.s.l. so that the maximal vertical distance of the forest limits for the entire investigation area is 1325 m (Table 1).

The TSA as equal positions for forests in the mountains were inferred from the forest lines and represent the total elevation belt from 1500 and 2900 m a.s.l. Except for the slope gradient diagram, the flat slope positions < 5° were additionally excluded from the TSA. The resulting TSA area is approximately 4975 km^2. In regard to the independent frequency distribution curves of the relief parameters in Fig. 4 between forest stands and the total TSA no statistical influence of the main topographic pattern on the forest distribution is detectable.

From the statistical point of view all four relief parameters control the forest distribution. Therefore, it is necessary to check the modelling accuracy of the PFA received from one single relief parameter against the combination of all four relief parameters (Table 2). Comparing the modelled PFA and the AFA four different classes can be built: (1) PFA with AFA and (2) no PFA without AFA are representing the mapped situation,

(3) PFA without AFA, and (4) no PFA with AFA are representing the differences between modelling and mapping. To receive a statistical background for the evaluation of the modelling quality of the delineated PFA, it is once related to the sum (FA_{AP}) of AFA and the PFA and twice referred to the total mountain area (TMA) of 8126 km^2, when the mountain boundary to the pediments of the foreland is generally defined by the changeover line of the slope gradient at 2.5°. From all four single relief parameters the modelling based on the slope aspect coincides best with the actual situation, but anyway the combination of all four parameters obviously enhances the prediction accuracy (Table 2). The PFA calculated from all 4 relief parameters is 1825 km^2 and therefore 3.5 times larger than the AFA. Figure 3 shows the spatial differences between the AFA and PFA. In relation to the AFA the PFA generally extends to the lower and upper elevations.

4.2 Forest line patterns

Figure 6 shows the lower forest line in the investigation area starting at 1600 m a.s.l. in the northwest and increasing to 2600 m a.s.l. in the southeast. Values for the lower forest line mostly are derived from the lower CAs but there are also many CAs in the higher elevations of the NFR, where the forest stands do not reach the valley bottom. This phenomenon may be caused by the local relief of tree free flat valley bottoms, which would be rather a climate than a topographic signal. But regarding the lower forest line in the second mountain range southeast of the intermountain basin and behind the NFR the lower forest line remains at a higher elevation around 2400 m a.s.l. Here the high lower forest line position is obviously caused by the drier climate conditions of the rain shadow position, which may also be true for the upper valleys in the NFR.

The upper forest line distribution and the area above the forest line are shown in Fig. 7. In the NFR the upper forest line at the mountain border starts in 1800 m a.s.l. in the west and increases to 2200 m a.s.l. in the east maintaining a vertical distance of 200 m to the lower forest line. From the mountain border in the north to the crest line the upper forest line rises to 2800 m a.s.l. and crossing the intermountain basin it lies in an elevation between 2400 and 2800 m a.s.l. in the SMR. The local vertical distance of the forest belt reaches its maximum value of more than 900 m at the northern side of the NFR. On the southern side and in the SMR the forest belt is very narrow with vertical distances between 50 and 400 m.

4.3 Climate environmental conditions

The environmental conditions were analysed in terms of frequency distribution of climate parameters for the AFA (Fig. 5) and were mapped together with the AFA (Figs. 8–10). The diagrams in Fig. 5 show the differences between AFA and TSA for all climate parameters except for the MAAT, which was already excluded as significant forest limitation parameter.

The lowest value class of forest stands for annual precipitation is 250 mm, while the highest potential evapotranspiration is up to 1100 mm a^{-1}. The difference between annual precipitation and evapotranspiration is an index for the potential water balance (pWB). One third of the AFA lies in areas with a negative pWB with values below 0 mm a^{-1} (Fig. 5) but with a precipitation amount between 300 and 700 mm a^{-1} (Fig. 8). These areas are specially situated at the westernmost edges and on the southern slopes of the mountain ranges. While the westernmost sites are exposed to the westerlies which transport most of the humidity, the southern slopes lie in the rain shadow but at a higher elevation and therefore the lower forest line is around 600 m higher than on the northern side of the NFR.

In the eastern part of the northern side of the NFR the AFA belt is very small and concurrently the lower forest line increases to 2000 m a.s.l., 400 m higher than in the western part of the NFR. Here the lower forest line occurs at precipitation of 700 mm and at positive pWB of 150 to 300 mm a^{-1}, while the PFA extends more into the lower slope positions which corresponds to the mean values of the regions described above. This is an indication for a non-natural distribution and points to greater human influence on forests in this region.

BGD
11, 14667–14698, 2014

The forest distribution related to mean air temperature in July ranges between 7 and 17 °C, with a maximum around 11 to 12 °C (Fig. 5). Comparing the AFA and PFA with the July-isotherms (Fig. 9), it can be seen that the upper AFA is mainly bordered by the 10 °C July-isotherm, but also extends to the 8 °C July-isotherm at many places. The upper PFA is generally combined with the 8 °C July-isotherm. Figure 10 shows the distribution of the monthly mean air temperature 5 °C isotherm during the growing season and the AFA. Except at the westernmost part the 5 °C isotherm is above the AFA between June and September and the upper AFA boundary coincides well with the 5 °C isotherm of September. The PFA at the upper forest boundary extends up to the position of 5 °C isotherm in June, where the growing season obviously becomes very short at these high elevated places. As shown in Figs. 9 and 10 the PFA at the upper limit is overestimated and the upper AFA boundary generally has a natural limitation.

5 Discussion and conclusions

It was shown that the AFA and the forest lines coincide well with the local climate conditions. At the lower limit forests are restricted to a minimum annual precipitation of 250 mm. The upper forest line is combined to the 10 °C July-isotherm in most places and to the minimum monthly mean temperature of 5 °C for the period between June and September. In the more humid parts of the investigation area at the western and northern slopes of the NFR both forest lines have a steep gradient and the forest belt has its greatest vertical extension between 500 and 600 m and locally up to 900 m. This fits well to the findings of increasing vertical forest extension concurrent with increasing humidity and vice versa by Fickert (1998), Dai et al. (2013), and Klinge et al. (2003) in the surrounding regions. Besides temperature, rainfall influences the upper forest line because clouds reduce the air temperature by shadowing and reflection of solar insulation. This is explaining the steep gradient of the upper forest line at the luv-side of the mountain ridges.

BGD
11, 14667–14698, 2014

The comparison of the AFA with climate data reveals a strong relation between the distribution patterns at the upper boundary but divergences occur at the lower boundary. This indicates human impact on the forests at the mountain borders modifying the lower forest line, while the upper forest line represents the natural condition. Accordingly the PFA derived from relief parameters at lower elevations indicates additional area for more potential natural forest. The PFA at the upper boundary is overestimated by highest forest stands occurring at few climate favoured places, because we used the total vertical distance of forest distribution as a relief parameter instead of the standard variation presuming that extensive logging may also occur in the alpine meadow pastures. GIS-analysis combined with multispectral satellite images and DTM is well suited to determine forest lines and potential forest areas for semi-arid regions in a local to regional scale. For forest line delineation it is necessary to eliminate elevation values which are restricted by the relief conditions and do not represent climatic limitations. DTM-derived relief parameters slope aspect, gradient and solar radiation serve well as indicators for the climatic environment in the investigation area and help to transfer environmental settings to other places in the broader study area. Human impact influences mainly the parameter elevation. Therefore a forest line evaluation with respect to the general climatic conditions has to be performed before the parameter elevation is incorporated into the spatial delineation process of the PFA. In conclusion, the proposed workflow is a helpful method for the evaluation of the potential forest distribution and the delineation of human impact. It can be used to indicate local climate variability, for landscape analysis and for effective reforestation planning.

Acknowledgements. The authors would like to thank the U.S. Geological Survey for making the satellite data free available for scientific research. We acknowledge support by the Open Access Publication Funds of the Goettingen University.

This Open Access Publication is funded by the University of Göttingen.

References

Böhner, J.: General climatic controls and topoclimatic variations of Central and High Mountain Asia, Boreas, 35, 279–295, 2006.

Böhner, J. and Antonic, O: Land-surface parameters specific to topo-climatology, in: Geomorphometry: Concepts, Software, Applications, Developments in Soil Science, edited by: Hengl, T. and Reuter, H. I., 33, 195–226, 2008.

Dai, L., Li, Y., Luo, G., Xu, W., Lu, L., Li, C., and Feng, Y.: The spatial variation of alpine timberlines and their biogeographical characteristics in the northern Tianshan Mountains of China, Environ Earth Science, 68, 129–137, doi:10.1007/s12665-012-1721-0, 2013.

Dulamsuren, C., Hauck, M., Khishigjargal, M., Leuschner, H. H., and Leuschner, C.: Diverging climate trends in Mongolian taiga forests influence growth and regeneration of *Larix sibirica*, Oecologia, 63, 1091–1102, doi:10.1007/s00442-010-1689-y, 2010.

Dulamsuren, C., Khishigjargal, M., Leuschner, C., and Hauck, M.: Response of tree-ring width to climate warming and selective logging in larch forests of the Mongolian Altai, J. Plant Ecol.-UK, 7, 24–38, doi:10.1093/jpe/rtt019, 2014.

Fickert, T.: Vergleichende Beobachtungen zu Solifluktions- und Frostmustererscheinungen im Westteil Hochasiens, Erlanger Geographische Arbeiten, 60, 150 pp., 1998.

Gerlitz, L., Bechtel, B., Zaksek, K., Kawohl, T., and Böhner, J.: SAGA GIS based processing of spatial high resolution temperature data, in: Proceedings of the 27. EnvironInfo-Conference 2013, 693–702, 2013.

Giese, E.: Wetterwirksamkeit atmosphärischer Zustände und Prozesse in Sowjet-Mittelasien, Westfälische Geographische Studien, 37, 395–410, 1973.

Giese, E.: Seßhaftwerden von Nomaden. Erfahrungen über die Dynamik traditioneller sozialer Einrichtungen (am Beispiel des kasachischen Volkes), in: Die Nomaden in Geschichte und Gegenwart. Beiträge zu einem internationalen Nomadismus-Symposium, Museum für Völkerkunde, Leipzig, 11–12 December 1975, Berlin, 175–197, 1981.

Giese, E.: Nomaden in Kasachstan – Ihre Seßhaftwerdung und Einordnung in das Kolchos- und Sowchossystem, Geographische Rundschau, 11, 575–588, 1983.

Haase, G., Richer, H., and Barthel, H.: Zum Problem landschaftsökologischer Gliederung, dargestellt am Beispiel des Changai-Gebirges in der Mongolischen Volksrepublik, Wissenschaftliche Veröffentlichungen d. Deutschen Instituts f. Länderkunde, 21/22, 489–516, 1964.

BGD
11, 14667–14698, 2014

Modelling forest lines and forest distribution patterns

M. Klinge et al.

Hansen, M. C., Potapov, P. V., Moore, R., Hancher, M., Turubanova, S. A., Tyukavina, A., Thau, D., Stehman, S. V., Goetz, S. J., Loveland, T. R., Kommareddy, A., Egorov, A., Chini, L., Justice, C. O., and Townshend, J. R. G.: High-resolution global maps of 21st-century forest cover change, Science, 342, 850–853, doi:10.1126/science.1244693, 2013.

Hilbig, W.: The Vegetation of Mongolia, Amsterdam, 258 pp., 1995.

Holdridge, L. R.: Determination of world plant formations from simple climatic data, Science, 105, 367–368, 1947.

Holtmeier, F.-K.: Die Höhengrenze der Gebirgswälder, Arbeiten aus dem Institut für Landschaftsökologie, 8, 337 pp., 2000.

Hövermann, J.: Das System der klimatischen Geomorphologie auf landschaftskundlicher Grundlage, Z. Geomorphol., 56, 143–153, 1985.

Jobbagy, E. G. and Jackson, R. B.: Global controls of forest line elevation in the northern and Southern Hemispheres, Global Ecol. Biogeogr., 9, 253–268, 2000.

Karger, A.: Historisch-geographische Wandlungen der Weidewirtschaft in den Trockengebieten der Sowjetunion am Beispiel Kasachstans, in: Weide-Wirtschaft in Trockengebieten, edited by: Knapp, R., Gießen, 37–49, 1965.

Kastner, M.: Patterns of forest distribution in Western Mongolia, Berliner Geowissenschaftliche Abhandlungen, A 205, 67–71, 2000.

Klinge, M., Böhner, J., and Lehmkuhl, F.: Climate patterns, snow- and timberlines in the Altai Mountains, Central Asia, Erdkunde, 57, 296–308, 2003.

Körner, C.: Alpine Treelines, Functional Ecology of the Global High Elevation Tree Limits, Springer, Basel, 220 pp., 2012.

Körner, C. and Paulsen, J.: A world-wide study of high altitude treeline temperatures, J. Biogeogr., 31, 713–732, 2004.

Liu, H., Williams, A. P., Allen, C. D., Guo, D., Wu, X., Anenkhonov, O. A., Liang, E., Sandanov, D. V., Yin, Y., Qi, Z., and Badmaeva, N. K.: Rapid warming accelerates tree growth decline in semi-arid forests of Inner Asia, Glob. Change Biol., 19, 2500–2510, doi:10.1111/gcb.12217, 2013.

Lydolph, P. E.: Climates of the Soviet Union, World Survey of Climatology, vol. 7, Amsterdam, 443 pp., 1977.

Machalett, B., Frechen, M., Hambach, U., Oches, E. A., Zöller, L., and Markovic, S. B.: The loess sequence from Remisowka (northern boundary of the Tien Shan Moun-

tains, Kazakhstan) – Part I: Luminescence dating, Quatern. Int., 152–153, 192–201, doi:10.1016/j.quaint.2005.12.014, 2006.
Mayer, T. and Bussemer, S.: Die Waldsteppe Südsibiriens. Ökosystemanalyse mit Hilfe der Radarfernerkundung, Mitteilungen der Geographischen Gesellschaft in München, 85, 161–180, 2001.
Medeu, A. R.: The National Atlas of the Republic of Kazakhstan/Institute of Geography. Part 1: Natural Conditions and Resources, Almaty, 150 pp., 2010.
Miehe, G. and Miehe, S.: Comparative high mountain research on the treeline ecotone under human impact, Erdkunde, 54, 34–50, 2000.
Miehe, G., Miehe, S., Koch, K., and Will, M.: Sacred forests in Tibet – using geographical information systems for forest rehabilitation, Mt. Res. Dev., 23, 324–328, 2003.
Miehe, G., Miehe, S., Will, M., Opgenoorth, L., Duo, L., Dorgeh, T., and Liu, J.: An inventory of forest relicts in the pastures of Southern Tibet (Xizang A. R., China), Plant Ecol., 194, 157–177, doi:10.1007/s11258-007-9282-0, 2008.
Paulsen, J. and Körner, C.: A climate-based model to predict potential treeline position around the globe, Alpine Botany, 124, 1–12, doi:10.1007/s00035-014-0124-0, 2014.
Rabus, B., Eineder, M., Roth, A., and Bamler, R.: The shuttle radar topography mission – a new class of digital elevation models acquired by spaceborne radar, ISPRS J. Photogramm., 57, 241–262, 2003.
Schlütz, F., Dulamsuren, C., Wieckowska, M., Mühlenberg, M., and Hauck, M.: Late Holocene vegetation history suggests natural origin of steppes in the northern Mongolian mountain taiga, Palaeogeogr. Palaeocl., 261, 203–217, 2008.
Soria-Auza, R. W., Kessler, M., Bach, K., Barajas-Barbosa, P. M., Lehnert, M., Herzog, S. K., and Böhner, J.: Impact of the quality of climate models for modelling species occurrences in countries with poor climatic documentation: a case study from Bolivia, Ecol. Model., 221, 1221–1229, 2010.
Treter, U.: Gebirgs-Waldsteppe in der Mongolei, Geographische Rundschau, 48, 655–661, 1996.
Treter, U.: Recent extension and regeneration of the larch forest in the mountain forest steppe of north-west Mongolia, Marburger Geographische Schriften, 135, 156–170, 2000.
Troll, C.: The upper timberlines in different climate zones, Arctic Alpine Res., 5, A3–A18, 1973a.
Troll, C.: High mountain belts between the polar caps and the equator: their definition and lower limit, Arctic Alpine Res., 5, A19–A27, 1973b.

BGD
11, 14667–14698, 2014

Modelling forest lines and forest distribution patterns

M. Klinge et al.

Title Page
Abstract | Introduction
Conclusions | References
Tables | Figures
◂◂ | ▸▸
◂ | ▸
Back | Close
Full Screen / Esc
Printer-friendly Version
Interactive Discussion

von Humboldt, A.: Kosmos: Entwurf einer physischen Weltbeschreibung, 5 volumes, Stuttgart, 1847–1862.
Walter, H. and Breckle, S. W.: Spezielle Ökologie der Gemäßigten und Arktischen Zonen Euro-Nordasiens, Ökologie der Erde, 3, Jena, 726 pp., 1994.
Wang, T., Ren, H., and Ma, K.: Climatic signals in tree ring of *Picea schrenkiana* along an altitudinal gradient in the central Tianshan Mountains, northwestern China, Trees, 19, 735–741, doi:10.1007/s00468-005-0003-9, 2005.
Wang, T., Zhang, Q. B., and Ma, K.: Treeline dynamics in relation to climatic variability in the central Tianshan Mountains, northwestern China, Global Ecol. Biogeogr., 15, 406–415, 2006.

BGD
11, 14667–14698, 2014

Modelling forest lines and forest distribution patterns

M. Klinge et al.

Table 1. Statistical values of the relief parameters related to the forest distribution.

Parameter	Unit	Maximum distribution value	Total distribution range	95 % of the distribution range
Elevation	m a.s.l.	2500	1575–2900	1925–2775
Aspect	degree horizontal	315 (NW)	0–360	260–70
Slope gradient	degree vertical	28	0–62	12–38
Solar radiation input	$kWh\,m^{-2}$	1075	450–1550	800–1325

BGD
11, 14667–14698, 2014

BGD
11, 14667–14698, 2014

Table 2. Comparison between of the modelled area values of single relief parameter classes and of the combination of all four relief parameters (AFA = actual forest area, PFA = potential forest area).

relief parameter:	elevation			solar radiation input			slope gradient			slope aspect			all 4 parameters		
site classification	km^2	% FA_{AP}	% TMA	km^2	% FA_{AP}	% TMA	km^2	% FA_{AP}	% TMA	km^2	% FA_{AP}	% TMA	km^2	% FA_{AP}	% TMA
(3) PFA without AFA	5358.7	91.4	65.9	4791.2	90.5	59.0	4279.9	89.5	52.7	3850.5	88.5	47.4	1323.6	72.5	16.3
(1) PFA with AFA	502.0	8.6	6.2	480.5	9.1	5.9	483.8	10.1	6.0	474.2	10.9	5.8	446.7	24.5	5.5
(4) No PFA with AFA	0.3	0.004	0.003	21.5	0.4	0.3	18.0	0.4	0.2	27.9	0.6	0.3	55.4	3.0	0.7
(2) No PFA without AFA	2265.2		27.9	2832.9		34.9	3344.4		41.2	3773.6		46.4	6300.7		77.5
Sum of all classifications which represent the actual situation	2767.2		34.1	3313.4		40.8	3828.3		47.1	4247.8		52.3	6747.4		83.0

% FA_{AP} = percent portion of the total actual and potential forest area.
% TMA = percent portion of total mountain area with 8126 km^2.

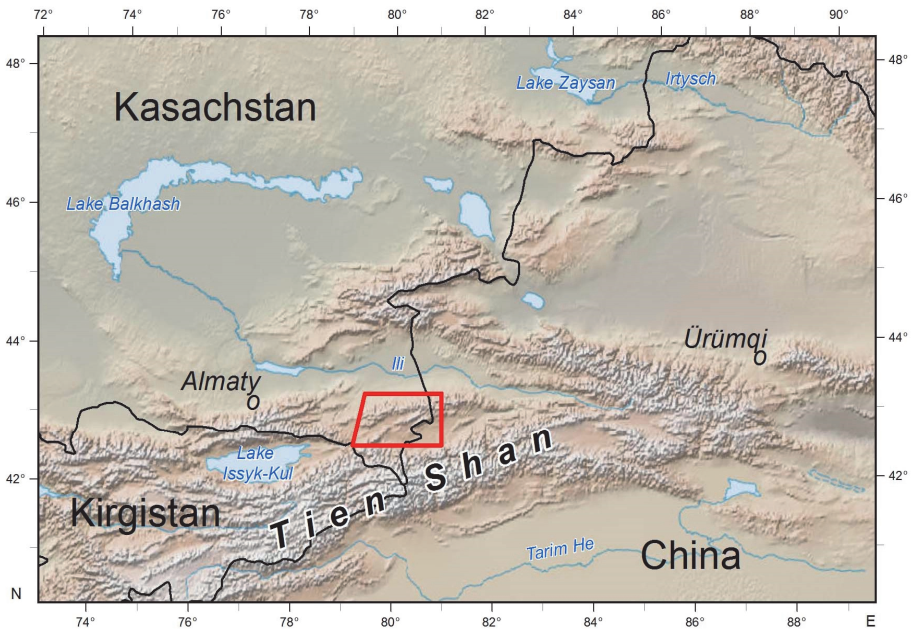

Figure 1. Map overview showing the detailed investigation area (rectangle) in Central Asia.

BGD
11, 14667–14698, 2014

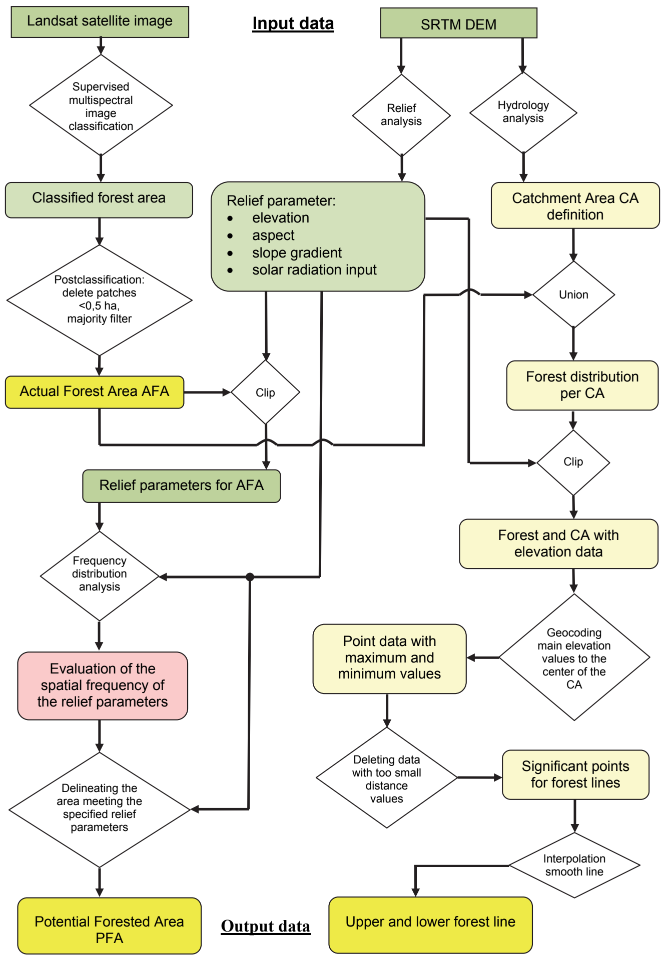

Figure 2. Workflow of DEM and satellite image processing to determine the spatial forest distribution patterns in semi-arid Mountain systems of Central Asia in a high resolution scale.

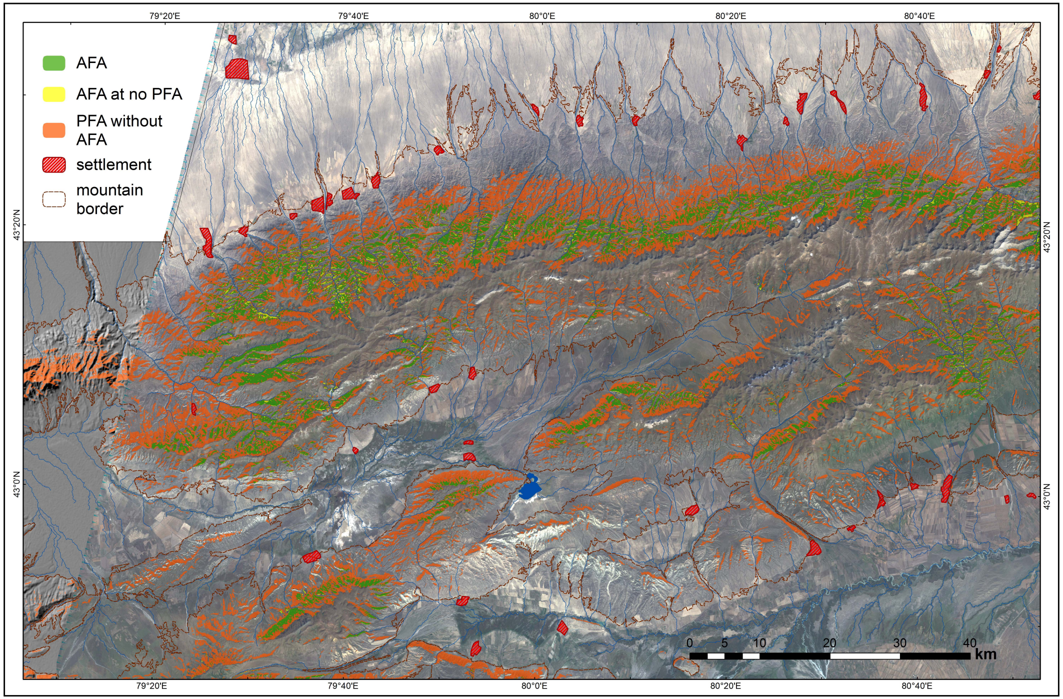

Figure 3. Spatial distribution of actual forested area AFA and potential forest area PFA in the mountainous region of northernmost Tien Shan shown above a true colour composite of a Landsat 7 satellite image of the 13 September 2000.

BGD
11, 14667–14698, 2014

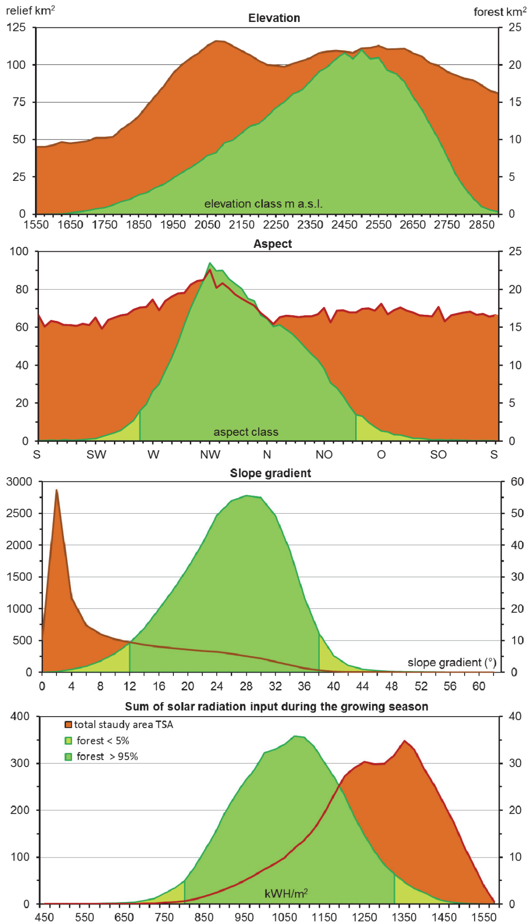

Figure 4. Frequency distribution of relief parameters in relation to actual forest area AFA (dark green = SD 95 %, light green = marginal value range excluded from PFA delineation) and total study area (TSA, brown).

BGD
11, 14667–14698, 2014

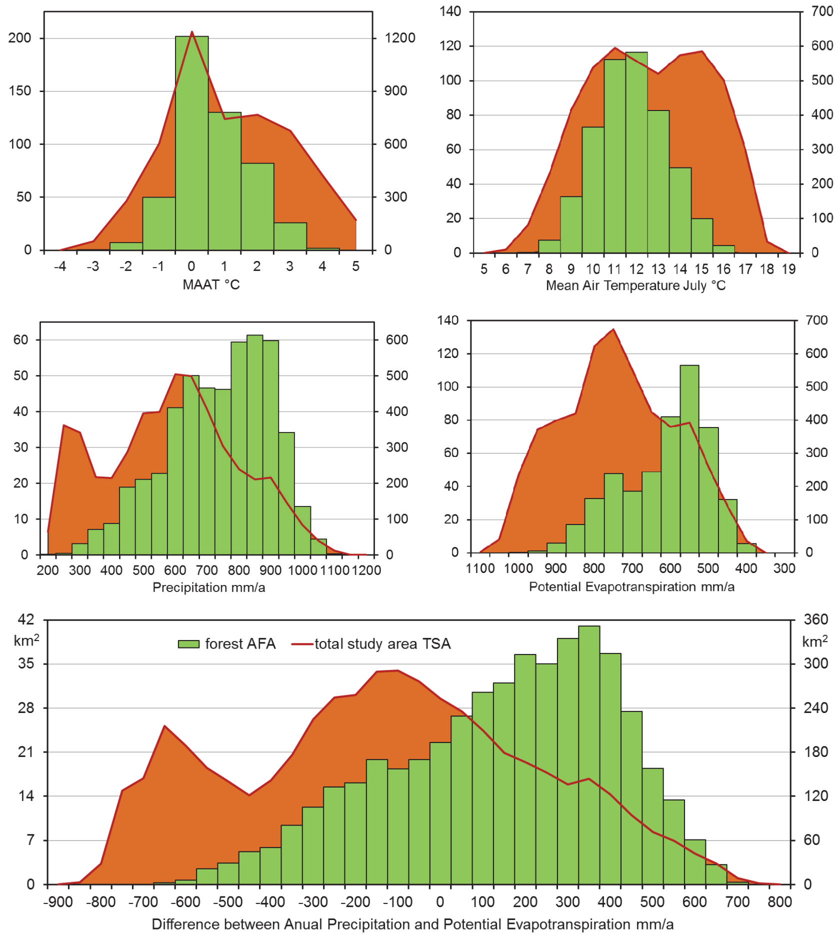

Figure 5. Frequency distribution of climate parameters for actual forest area (AFA, columns, left axes km^2) and the total study area (TSA, graph, right axes km^2).

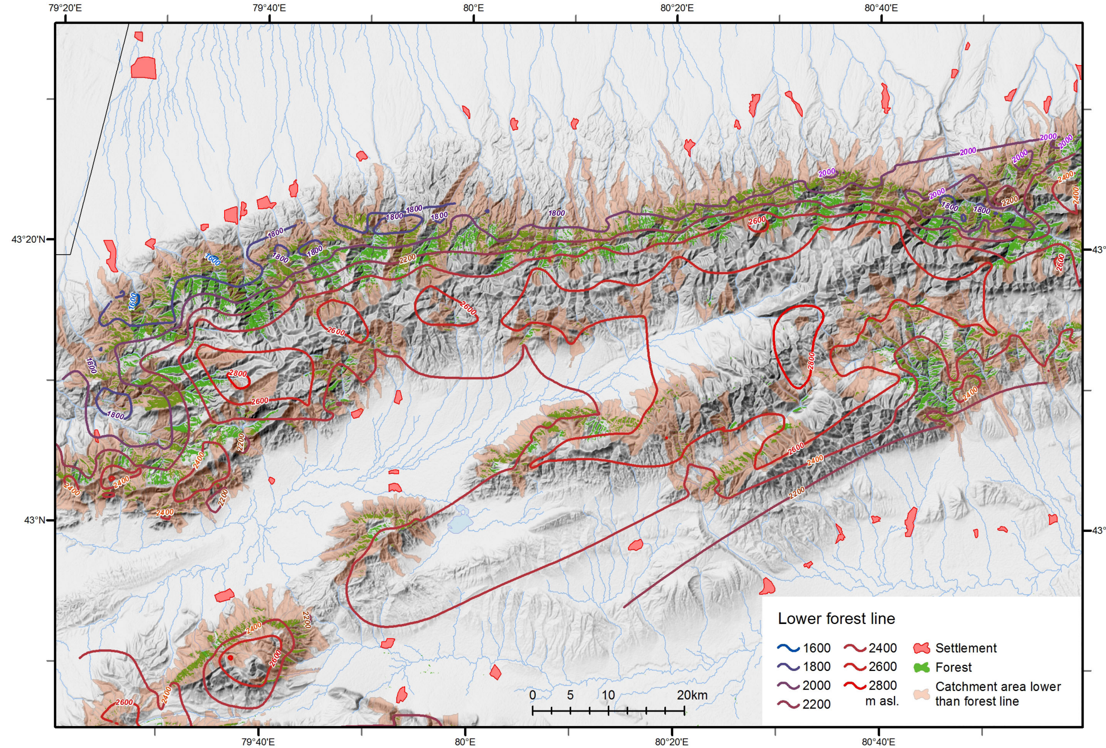

Figure 6. The lower forest line and the catchment areas providing lower forest line values in the investigation area.

BGD
11, 14667–14698, 2014

Modelling forest lines and forest distribution patterns

M. Klinge et al.

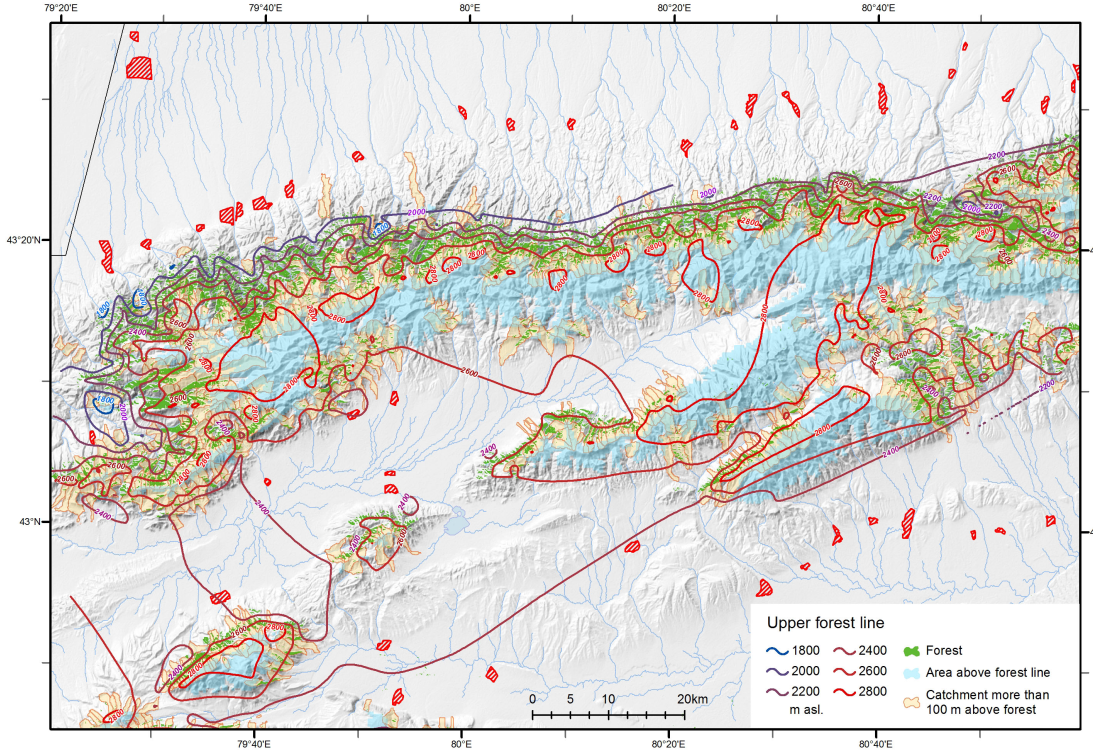

Figure 7. The upper forest line and the catchment areas providing upper forest line values in the investigation area.

BGD
11, 14667–14698, 2014

Modelling forest lines and forest distribution patterns

M. Klinge et al.

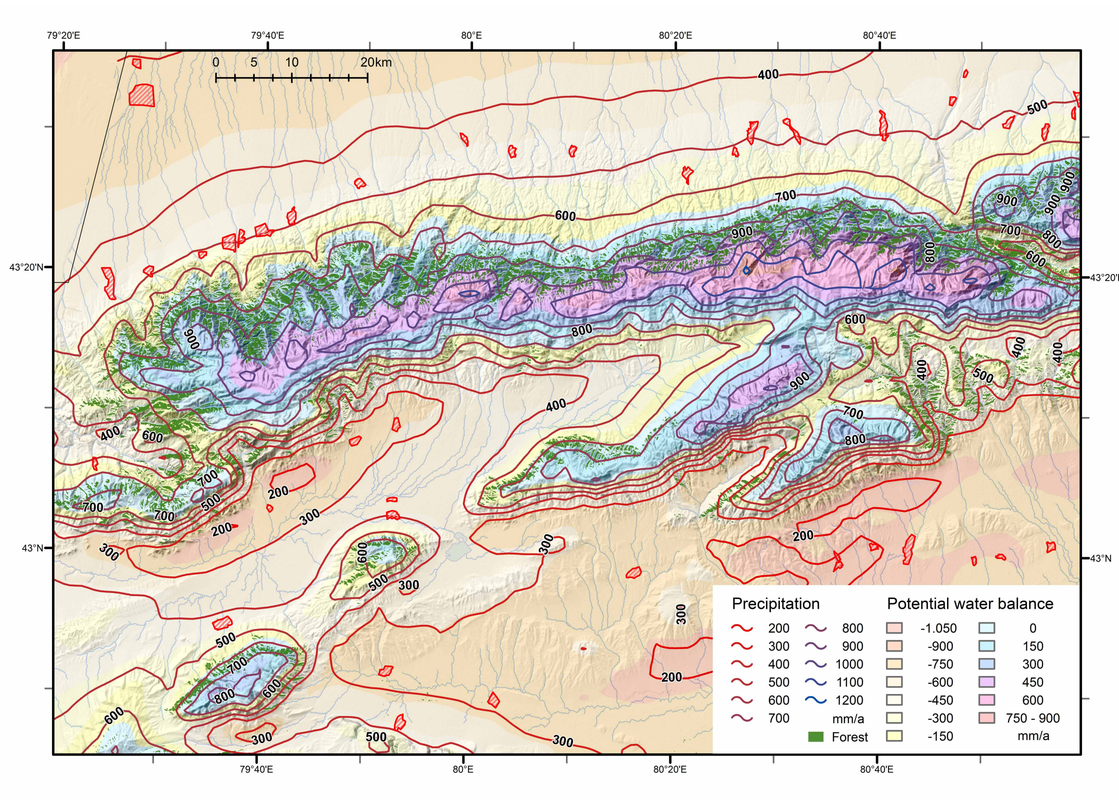

Figure 8. Forest distribution AFA in relation to the hydrological climatic environment.

BGD
11, 14667–14698, 2014

Modelling forest lines and forest distribution patterns

M. Klinge et al.

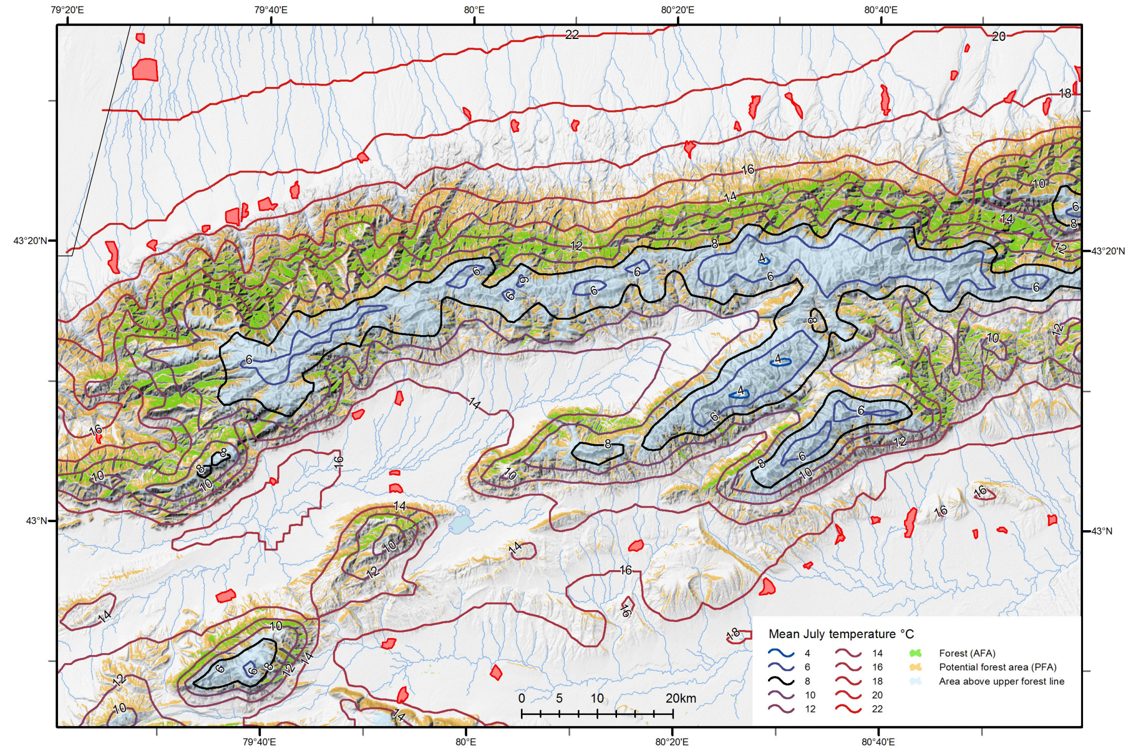

Figure 9. Forest distribution AFA and PFA and the July isotherms.

BGD

11, 14667–14698, 2014

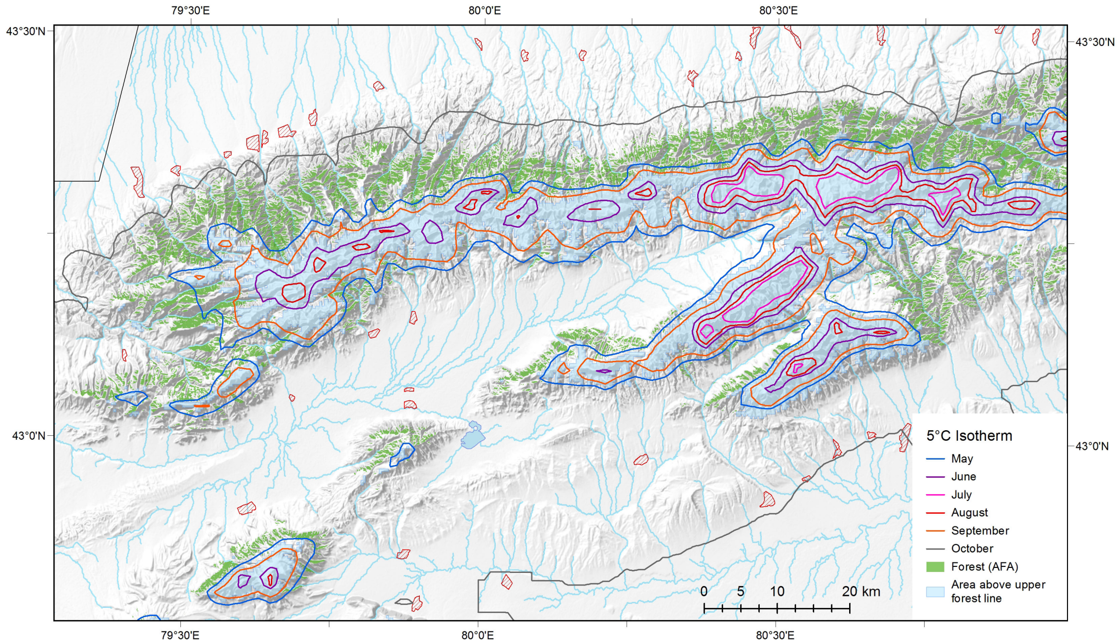

Figure 10. Forest distribution AFA and the 5 °C monthly isotherms during the growing season.

BGD
11, 14667–14698, 2014